Article

Discovery Medicine 2026; 38(207): 1195–1209
https://doi.org/10.24976/Discov.Med.202638207.95

A Novel Nomogram Based on ALBI Grade and Dynamic SII for Predicting Prognosis of Unresectable HCC Treated With TACE Plus Toripalimab

Yanjun Pu[1], Fen He[2], Xuyin Wang[1], Tong Lu[1], Jing Wang[1,*]

[1]Department of Interventional and Vascular Surgery, People's Hospital of Ningxia Hui Autonomous Region, NingXia Medical University, 750002 Yinchuan, Ningxia, China
[2]Department of Otorhinolaryngology Head and Neck Surgery, People's Hospital of Ningxia Hui Autonomous Region, NingXia Medical University, 750002 Yinchuan, Ningxia, China
*Correspondence: yunwj3133@163.com (Jing Wang)
Submitted: 25 February 2026 Revised: 11 March 2026 Accepted: 28 March 2026 Published: 20 April 2026

Background: Outcomes of transarterial chemoembolization (TACE) combined with programmed cell death-1 (PD-1) inhibitors for unresectable hepatocellular carcinoma (HCC) remain heterogeneous. This study evaluated the prognostic value of the dynamic Systemic Immune-Inflammation Index (Delta SII) and Albumin-Bilirubin (ALBI) grade to construct a predictive nomogram.

Methods: We retrospectively analyzed 168 patients with unresectable HCC treated with TACE plus PD-1 inhibitors. Delta SII was defined as the relative change from baseline to the first follow-up. Independent prognostic factors for Overall Survival (OS) were identified via Cox regression to build a nomogram. Delta SII was categorized into High and Low groups using an optimal cut-off of 32.7%, determined by maximally selected rank statistics. Post-treatment SII (SII_T1) was measured within a prespecified window of 28–42 days post-treatment. The nomogram was internally validated using 500-bootstrap resampling, and performance was assessed by time-dependent Area Under the Curve (AUC) with 95% confidence intervals, calibration plots, and Decision Curve Analysis (DCA). All patients received toripalimab (240 mg every 3 weeks) as the PD-1 inhibitor.

Results: Patients with a High Delta-SII or ALBI Grade 2/3 exhibited significantly inferior OS and Progression-Free Survival (PFS) ($p < 0.001$). Multivariate analysis identified Tumor Size (Hazard Ratio (HR): 1.10, 95% CI: 1.04–1.16), Tumor Number (HR: 1.34, 95% CI: 1.10–1.63), macrovascular invasion (MVI) (HR: 1.64, 95% CI: 1.08–2.48), ALBI Grade 2/3 (HR: 2.76, 95% CI: 1.62–4.70), and High Delta-SII group (HR: 2.84, 95% CI: 1.86–4.33) as independent risk factors for mortality. The constructed nomogram demonstrated robust discrimination, with AUCs of 0.804 (95% CI: 0.737–0.872) for 1-year and 0.823 (95% CI: 0.756–0.890) for 2-year OS. Calibration curves showed excellent agreement between predicted and observed survival, and DCA confirmed the model's clinical utility.

Conclusion: The dynamic evolution of systemic inflammation (Delta SII) and baseline hepatic reserve (ALBI grade) are powerful synergistic predictors of survival in unresectable HCC patients receiving TACE plus PD-1 inhibitors. The proposed nomogram, which prioritizes host biological resilience over tumor burden alone, offers a precise and visual tool to guide clinical decision-making and identify patients most likely to benefit from this combination therapy.

Keywords: hepatocellular carcinoma; transarterial chemoembolization; PD-1 inhibitors; Systemic Immune-Inflammation Index; ALBI grade; prognosis; nomogram

Introduction

Hepatocellular carcinoma (HCC) remains a global health challenge, characterized by high mortality rates and frequent diagnosis at advanced stages where curative resection is precluded [1,2]. For patients with unresectable disease, transarterial chemoembolization (TACE) has historically served as the standard of care [3,4]. The therapeutic landscape has recently evolved with the advent of immune checkpoint inhibitors (ICIs), specifically programmed cell death-1 (PD-1) inhibitors [5,6]. The rationale for combining TACE with PD-1 blockade is synergistic. TACE induces ischemic tumor necrosis, releasing tumor-associated antigens that can overcome immune exclusion and enhance the systemic efficacy of ICIs [7]. Despite the promise of this combinatorial strategy, clinical responses exhibit significant heterogeneity [8]. This heterogeneity manifests across multiple dimensions: objective response rates (ORR) vary widely from approximately 20% to 60%, median overall survival (OS) ranges from less than 10 months to over 20 months across different cohorts, and a substantial proportion of patients experience early radiological progression within the first three months of treatment. Moreover, a non-

Copyright: © 2026 The Author(s). Published by Discovery Medicine. This is an open access article under the CC BY 4.0 license.
Note: *Discovery Medicine* stays neutral with regard to jurisdictional claims in published maps and institutional affiliations.

trivial subset of patients fail to derive meaningful survival benefits, succumbing to either rapid tumor progression or treatment-related hepatic decompensation.

Accurate prognostication is essential to optimize patient selection and avoid futile treatments. Traditional staging systems, such as the Barcelona Clinic Liver Cancer (BCLC) classification, rely heavily on tumor burden metrics, specifically tumor size and number, to dictate prognosis [9,10]. While effective for cytotoxic therapies, these anatomical models often overlook the complex host-tumor interactions that govern outcomes in the era of immunotherapy [11]. Emerging evidence suggests that the efficacy of PD-1 inhibitors depends less on tumor bulk and more on the host's functional physiological reserve, comprising both hepatic function and systemic immune status [12].

Furthermore, hepatic reserve is a decisive factor in the survival of HCC patients, influencing tolerance to therapeutic stress [13,14]. The Albumin-Bilirubin (ALBI) grade offers a strictly objective assessment of liver function, eliminating the subjective variability of ascites and encephalopathy inherent in the Child-Pugh score [15]. By relying solely on albumin and bilirubin levels, the ALBI grade provides a more granular stratification of hepatic resilience, which is particularly critical given the potential hepatotoxicity associated with TACE and immune-mediated adverse events [16].

Parallel to liver function, systemic inflammation is recognized as a hallmark of cancer progression [17]. The Systemic Immune-Inflammation Index (SII), calculated from platelet, neutrophil, and lymphocyte counts, integrates three independent inflammatory pathways into a single composite marker [18]. Neutrophils and platelets promote tumor progression via angiogenesis, immune evasion, and pro-metastatic niche formation. In contrast, lymphocytes mediate cytotoxic antitumor immunity [19]. An elevated SII typically signifies a dominance of pro-tumorigenic inflammation over host immune surveillance [20].

Most existing studies have focused on static baseline inflammatory markers. TACE, however, is an invasive procedure that induces acute ischemic hypoxia, triggering a surge in pro-inflammatory cytokines and vascular endothelial growth factor (VEGF) [21]. Current prognostic models, including the BCLC staging system, the Child-Pugh score, and existing static inflammatory indices such as baseline SII were all constructed from single time-point measurements and therefore inherently fail to account for this treatment-induced inflammatory fluctuation. For instance, the BCLC system focuses primarily on tumor morphology and performance status, while the Child-Pugh score captures a fixed snapshot of hepatic function; neither framework incorporates the longitudinal immune response triggered by the TACE procedure itself. This treatment-induced, iatrogenic inflammatory storm may paradoxically fuel tumor progression by fundamentally altering the immune microenvironment [22]. Consequently, static baseline values may fail to capture the host's dynamic physiological response to treatment. We hypothesize that the longitudinal evolution of the SII (dynamic Systemic Immune-Inflammation Index (Delta SII), reflecting the balance between treatment-induced inflammation and immune activation, serves as a superior prognostic surrogate compared to pretreatment values alone.

Currently, robust models integrating dynamic immune-inflammatory changes with objective hepatic reserve for this specific combination therapy are lacking. This study aimed to evaluate the prognostic value of ALBI grade and Delta SII in patients with unresectable HCC undergoing TACE plus PD-1 inhibitors. Based on these determinants, we constructed and validated a novel nomogram to provide clinicians with a visual and precise tool for survival prediction.

Methods

Study Design and Patient Population

This retrospective study analyzed data from patients diagnosed with unresectable HCC who received TACE combined with PD-1 inhibitor therapy at People's Hospital of Ningxia Hui Autonomous Region between January 2020 and January 2025.

The inclusion criteria were as follows: (1) clinically or pathologically confirmed HCC; (2) classification as unresectable HCC (BCLC stage B or C) according to current guidelines [23]; (3) treated with TACE combined with PD-1 inhibitors; (4) Child-Pugh class A or B; and (5) availability of complete medical records and follow-up data. Patients were excluded if they had: (1) concurrent malignancies; (2) severe dysfunction of vital organs (heart, lungs, or kidneys); (3) active autoimmune diseases; or (4) missing data for key laboratory indicators required to calculate ALBI or SII.

Treatment Protocol

TACE was performed by experienced interventional radiologists using the standard Seldinger technique. The choice of TACE modality (conventional TACE [cTACE] vs. drug-eluting bead TACE [DEB-TACE]) was based on tumor vascular anatomy and operator discretion. For cTACE, an emulsion of iodized oil (Lipiodol Ultra-Fluide, Guerbet, Villepinte, France) and cisplatin (Qilu Pharmaceutical Co., Ltd., Jinan, China; Jiangsu Hansoh Pharmaceutical Group Co., Ltd., Lianyungang, China) was selectively infused into tumor-feeding arteries, followed by embolization with gelatin sponge particles (Hangzhou Alc Co., Ltd., Hangzhou, China) or polyvinyl alcohol particles (Hangzhou Alc Co., Ltd., Hangzhou, China) until near-stasis was achieved. For DEB-TACE, commercially available drug-eluting beads (Jiangsu Hengrui Medicine Co., Ltd., Lianyungang, China) loaded with epirubicin (Shenzhen Main Luck Pharmaceuticals Inc., Shenzhen, China) were administered in accordance with the manu-

facturer's instructions and institutional practice. Superselective catheterization was attempted whenever feasible. Repeat TACE was considered based on imaging response, liver function, and patient tolerance. The number of TACE sessions during the study period was recorded (median [IQR]).

PD-1 inhibitors were initiated within 3–7 days after the first TACE procedure. In this cohort, toripalimab (240 mg/6 mL; Shanghai Junshi Biosciences Co., Ltd., Shanghai, China) was used as the PD-1 inhibitor, and dosing at 240 mg every 3 weeks followed the approved labeling and contemporary clinical guidelines. PD-1 therapy was continued until radiological progression, unacceptable toxicity, liver decompensation, or patient withdrawal. The total number of PD-1 cycles and the median treatment duration were documented. Concomitant anticancer treatments (e.g., tyrosine kinase inhibitors, radiotherapy, ablation, or other systemic agents) during follow-up were recorded and considered in the analysis.

Data Collection and Definitions

Baseline demographic and clinicopathological characteristics were collected, including age, gender, etiology, Eastern Cooperative Oncology Group performance status (ECOG PS), tumor size, tumor number, macrovascular invasion (MVI), extrahepatic spread (EHS), and laboratory parameters. The final analytical dataset contained no missing values across all variables (missing rate = 0% for all 30 variables), as complete laboratory data availability was a mandatory inclusion criterion.

Calculation of ALBI Grade and SII

The ALBI score was calculated using the following formula based on baseline laboratory data: ALBI score = ($\log_{10}$(bilirubin [μmol/L]) × 0.66) – (albumin [g/L] × 0.085). Patients were stratified into three grades: Grade 1 (<–2.60), Grade 2 (≥–2.60 to <–1.39), and Grade 3 (≥–1.39). In our cohort, no patients met the criteria for Grade 3; consequently, the binary categorization of Grade 1 versus Grade 2/3 is de facto equivalent to Grade 1 versus Grade 2 in the present analysis.

The SII was calculated using routine complete blood count data as: SII = (Platelet count [10^9/L] × Neutrophil count [10^9/L]) / Lymphocyte count [10^9/L]. Baseline SII (SII_T0) was obtained from blood samples collected at the first TACE procedure. Post-treatment SII (SII_T1) was obtained from blood samples collected at the first schedule follow-up visit within the prespecified window of 28–42 days after the initial treatment. The dynamic change in SII (Delta SII) was defined as the proportional change relative to the baseline value: Delta SII = (SII_T1 – SII_T0) / SII_T0 × 100%. A positive Delta SII value indicates an increase in systemic immune-inflammatory burden following treatment, whereas a negative value indicates a reduction. The optimal cut-off value for Delta SII was determined using maximally selected rank statistics (using the "surv_cutpoint" function in the survminer R package version 0.4.9), which identifies the threshold that maximizes the standardized log-rank statistic. The derived optimal cut-off value was 32.7%. Based on this threshold, 60 patients (35.7%) were classified into the High Delta-SII group (Delta SII > cut-off) and 108 patients (64.3%) into the Low Delta-SII group (Delta SII ≤ cut-off). The distribution of Delta SII values and the corresponding cut-off are illustrated in **Supplementary Fig. 1**. To minimize timing-related variability, the first follow-up blood test (SII_T1) was defined within a prespecified window of 28–42 days after the initial treatment; if multiple tests were available within the window, the test closest to day 35 was used. This window was further supported by the pharmacokinetic profile of toripalimab, which has a reported elimination half-life exceeding 20 days; drug concentrations and PD-1 receptor occupancy therefore remain relatively stable throughout the 28–42 day interval, ensuring that SII_T1 reflects the cumulative immunobiological response to both TACE-induced ischemia and two cycles of PD-1 inhibition, rather than an acute peri-infusion transient. This window was selected to ensure that all patients had received exactly two doses of toripalimab prior to sampling (administered on Day 0 and Day 21), while avoiding the acute peri-infusion immune activation transient that typically resolves within 7 days of each infusion. Patients with overt acute infection or hematologic conditions at the time of blood sampling (e.g., fever requiring antibiotics, active gastrointestinal bleeding, or steroid pulse therapy) were excluded.

The histogram illustrates the distribution of Delta SII values across all 168 patients included in the analysis. Delta SII was defined as the proportional change in the Systemic Immune-Inflammation Index from baseline (SII_T0) to the first follow-up assessment (SII_T1), calculated as (SII_T1 – SII_T0) / SII_T0 × 100%. The optimal cut-off value (32.7%) was determined using the maximally selected rank statistics method (surv_cutpoint function, survminer R package), which identifies the threshold that maximizes the standardized log-rank statistic for overall survival. The red dashed vertical line indicates the optimal cut-off. Patients with Delta SII values exceeding this threshold were classified into the High Delta-SII group (red bars; n = 60, 35.7%), while those at or below the threshold were classified into the Low Delta-SII group (blue bars; n = 108, 64.3%). Abbreviations: SII, Systemic Immune-Inflammation Index; Delta SII, dynamic change in SII.

Follow-up and Endpoints

Patients were followed up regularly every 4–8 weeks. The primary endpoints were overall survival (OS) and Progression-Free Survival (PFS). OS was defined as the time from the first TACE–PD-1 treatment to death from any cause or the last follow-up. PFS was defined as the time from the first TACE–PD-1 treatment to radio-

logical progression (assessed according to mRECIST) or death, whichever occurred first. Radiological progression was independently assessed by two experienced radiologists with hepatic imaging subspecialty expertise using contrast-enhanced CT (uCT 760, United Imaging Healthcare, Shanghai, China) or MRI (uMR 780, United Imaging Healthcare, Shanghai, China) according to mRECIST criteria; discordant interpretations were resolved by consensus discussion within the institutional multidisciplinary team. As this was a retrospective study, evaluations were not performed under formally blinded conditions. The data cut-off date was June 30, 2025. During follow-up, 97 deaths and 125 progression events were observed. The median follow-up duration was 39.3 months, estimated using the reverse Kaplan–Meier method (based on OS follow-up). For administrative consistency, follow-up was capped at 60 months for patients who remained alive and event-free at that landmark; these patients are reflected as administratively censored observations in the survival analyses.

Statistical Analysis

All statistical analyses were performed using R software (version 4.5.2, R Foundation for Statistical Computing, Vienna, Austria). Missing data were handled using complete-case analysis (patients with missing key variables were excluded from modeling). Continuous variables were expressed as median [interquartile range, IQR] and compared using the Wilcoxon rank-sum test. Categorical variables were presented as frequencies (percentages) and compared using the Chi-square test or Fisher's exact test. To evaluate potential information loss from dichotomization of Delta SII, we performed sensitivity analyses using Delta SII as a continuous linear term and as a restricted cubic spline (RCS, 4 knots) in the multivariable Cox model. The nonlinearity test was non-significant ($p = 0.172$), and the C-index of the continuous model (0.752) was virtually identical to that of the binary model (0.752). Although the continuous model achieved a marginally lower AIC (834.54 vs 837.86 for the binary model), this marginal improvement in model fit did not translate into any gain in discriminative performance.

Formal a priori sample size calculation was not performed given the retrospective nature of this study; however, the adequacy of the sample size was evaluated post hoc using the Events Per Variable (EPV) criterion. The multivariate Cox regression model included five independent predictors, and 97 mortality events were observed during follow-up, yielding an EPV of approximately 19.4. This substantially exceeds the commonly recommended minimum threshold of 10 EPV, supporting the statistical stability and reliability of the multivariable model. Furthermore, the use of 500-bootstrap internal validation was employed to mitigate potential overfitting arising from the limited sample size.

Survival curves were generated using the Kaplan-Meier method and compared using the Log-rank test. Univariate and multivariate Cox proportional hazards regression analyses were performed to identify independent prognostic factors. Given the right-skewed distribution of AFP values (range: 22–1516 ng/mL), a $\log_{10}$ transformation was applied prior to Cox regression analysis to address potential scale effects. Variables with $p < 0.10$ in univariable analysis and/or clinically relevant covariates were considered for multivariable modeling. Multicollinearity among covariates was assessed using the Variance Inflation Factor (VIF). Specifically, to avoid statistical redundancy, composite scores (e.g., ALBI grade) and their constituent components (e.g., albumin and total bilirubin) were not entered into the multivariate model simultaneously. The proportional hazards assumption was assessed using Schoenfeld residuals.

Based on the independent predictors identified in the multivariate analysis, a prognostic nomogram was constructed to predict 1- and 2-year OS probabilities. The nomogram performance was assessed using three complementary methods. First, discrimination was evaluated by the area under the time-dependent ROC curve (AUC). Time-dependent AUC values were calculated using the inverse probability of censoring weighting (IPCW) method via the timeROC package (version 0.4), which appropriately accounts for patients censored prior to each time point of interest by upweighting the contributions of uncensored observations. Second, calibration was assessed using calibration plots comparing predicted versus observed survival probabilities, with 500 bootstrap resamples for internal validation. Third, clinical utility was evaluated by Decision Curve Analysis (DCA), which quantified the net benefit of the model across a range of threshold probabilities. A two-sided p-value < 0.05 was considered statistically significant.

This study was conducted in accordance with the Declaration of Helsinki and was approved by the Institutional Review Board (IRB) of People's Hospital of Ningxia Hui Autonomous Region (Approval No. [2025]-NZR-229). Given the retrospective nature of the study and the use of anonymized clinical data, the requirement for written informed consent was waived. The study is reported in line with the STROBE statement for observational studies and the TRIPOD guideline for prognostic model development and validation.

Results

Patient Characteristics

The baseline characteristics of the 168 enrolled patients are listed in Table 1. The study population was categorized into Low Delta-SII (n = 108) and High Delta-SII (n = 60) groups. Statistical analysis revealed that the High Delta-SII group was associated with a heavier tumor burden

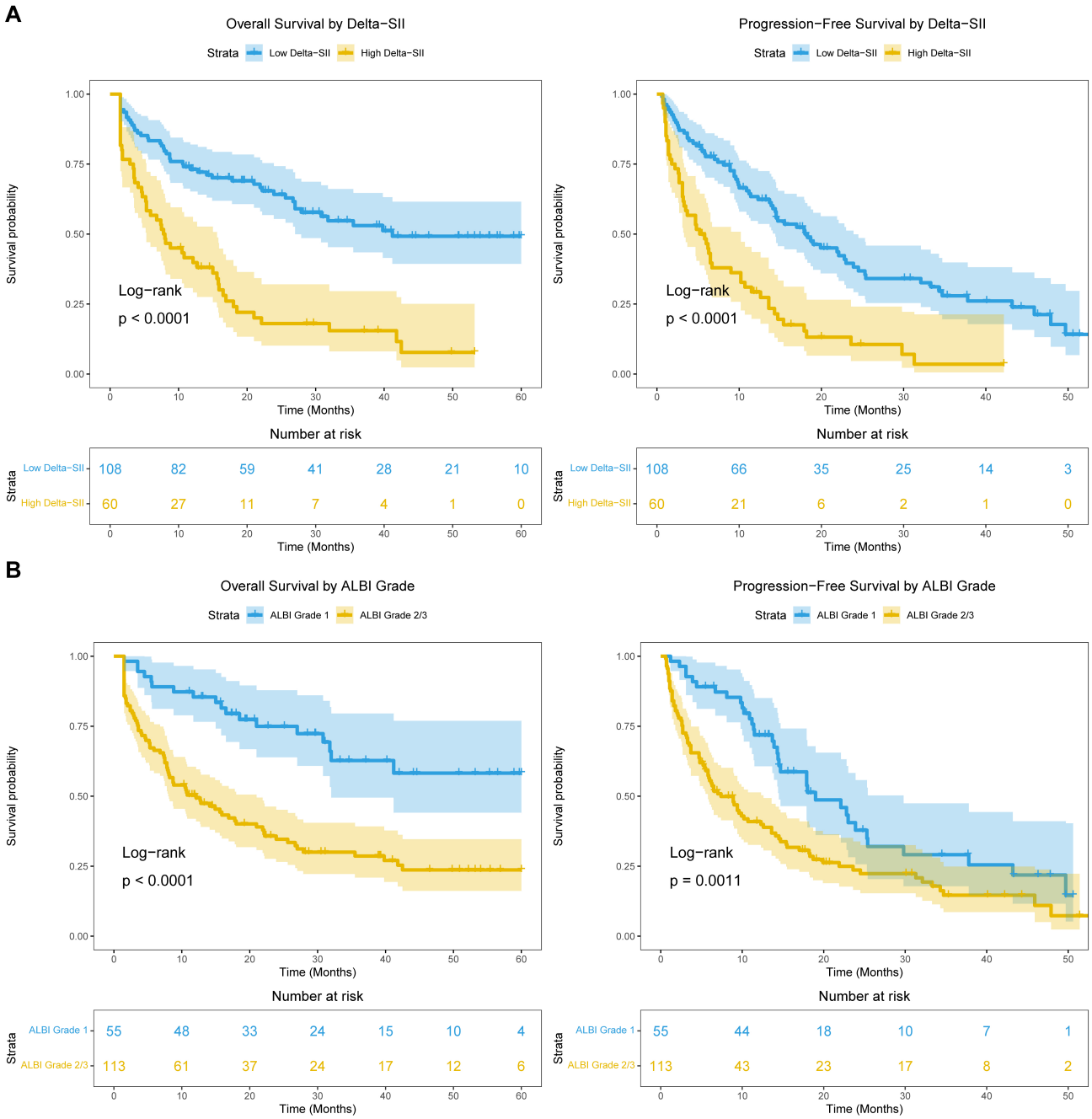

Fig. 1. Kaplan-Meier survival curves for Overall Survival (OS) and Progression-Free Survival (PFS). (A) Survival curves stratified by Delta SII groups (Low vs. High). Patients with Low Delta-SII (blue line) showed significantly better OS ($p < 0.0001$) and PFS ($p < 0.0001$) compared to the High Delta-SII group (yellow line). (B) Survival curves stratified by ALBI grade (Grade 1 vs. Grade 2/3). Patients with ALBI Grade 1 (blue line) demonstrated significantly longer OS ($p < 0.0001$) and PFS ($p = 0.0011$) than those with ALBI Grade 2/3 (yellow line). *p*-values were calculated using the Log-rank test. Shaded areas represent 95% confidence intervals. Abbreviations: SII, Systemic Immune-Inflammation Index; ALBI, Albumin-Bilirubin grade.

and compromised hepatic function compared to the Low Delta-SII group. Specifically, patients with elevated Delta SII had larger tumor diameters ($p = 0.008$) and worse liver reserve, indicated by higher total bilirubin ($p < 0.001$) and ALBI grade ($p = 0.011$). Of note, baseline SII levels were comparable between the groups ($p = 0.886$), suggesting that the dynamic change in SII, rather than the static baseline value, correlates with specific clinical features. No significant differences were found in other demographics or tumor characteristics such as MVI and AFP levels.

Table 1. Baseline demographic and clinicopathological characteristics of patients with unresectable HCC stratified by Delta SII.

	Low	High	Overall	*p*-value
	(N = 108)	(N = 60)	(N = 168)	
Age (years)				0.931
Median [IQR]	57 [50, 66]	58 [49, 68]	57 [50, 67]	
Gender				1.000
Female	20 (18.5%)	11 (18.3%)	31 (18.5%)	
Male	88 (81.5%)	49 (81.7%)	137 (81.5%)	
Etiology				0.674
HBV	57 (52.8%)	35 (58.3%)	92 (54.8%)	
HCV	24 (22.2%)	10 (16.7%)	34 (20.2%)	
Other	27 (25.0%)	15 (25.0%)	42 (25.0%)	
ECOG Performance Status				0.229
0	68 (63.0%)	44 (73.3%)	112 (66.7%)	
1	40 (37.0%)	16 (26.7%)	56 (33.3%)	
Tumor Size (cm)				0.008
Median [IQR]	5.6 [3.1, 8.4]	7.0 [4.8, 9.6]	5.9 [4.2, 8.8]	
Tumor Number				0.81
Median [IQR]	3.0 [2.0, 3.0]	3.0 [2.0, 4.0]	3.0 [2.0, 3.0]	
Macrovascular Invasion (MVI)				0.633
No	65 (60.2%)	33 (55.0%)	98 (58.3%)	
Yes	43 (39.8%)	27 (45.0%)	70 (41.7%)	
Extrahepatic Spread (EHS)				0.375
No	77 (71.3%)	47 (78.3%)	124 (73.8%)	
Yes	31 (28.7%)	13 (21.7%)	44 (26.2%)	
AFP (ng/mL)				0.083
Median [IQR]	107 [72, 200]	139 [91, 220]	123 [76, 206]	
ALT (U/L)				0.162
Median [IQR]	35 [23, 54]	29 [16, 46]	33 [19, 52]	
AST (U/L)				0.161
Median [IQR]	37 [21, 57]	43 [26, 78]	38 [23, 60]	
Total Bilirubin (umol/L)				<0.001
Median [IQR]	6.0 [5.0, 18.5]	16.9 [5.0, 78.5]	9.8 [5.0, 33.4]	
Albumin (g/L)				0.938
Median [IQR]	38 [35, 42]	38 [35, 41]	38 [35, 41]	
ALBI_Grade				0.011
Grade 1	43 (39.8%)	12 (20.0%)	55 (32.7%)	
Grade 2/3	65 (60.2%)	48 (80.0%)	113 (67.3%)	
Baseline SII				0.886
Median [IQR]	460 [300, 580]	440 [320, 620]	460 [300, 590]	

Data are presented as number (percentage) for categorical variables and median [interquartile range] for continuous variables. *p*-values were calculated using the Chi-square test or Fisher's exact test for categorical variables, and the Wilcoxon rank-sum test for continuous variables. A p-value < 0.05 indicates statistical significance. Abbreviations: SII, Systemic Immune-Inflammation Index; IQR, Interquartile Range; HBV, Hepatitis B Virus; HCV, Hepatitis C Virus; ECOG PS, Eastern Cooperative Oncology Group Performance Status; MVI, Macrovascular Invasion; EHS, Extrahepatic Spread; AFP, Alpha-fetoprotein; ALT, Alanine Aminotransferase; AST, Aspartate Aminotransferase; ALBI, Albumin-Bilirubin.

Survival Outcomes Stratified by Delta SII and ALBI Grade

The Kaplan-Meier survival analysis was performed to evaluate the prognostic value of Delta SII and ALBI grade. As shown in Fig. 1A, patients in the High Delta-SII group exhibited significantly inferior outcomes compared to those in the Low Delta-SII group. The High Delta-SII group was associated with a markedly shorter Overall Survival (OS) ($p < 0.0001$) and Progression-Free Survival (PFS) ($p < 0.0001$). Similarly, the baseline hepatic reserve, assessed

Table 2. Univariate and multivariate Cox proportional hazards' regression analysis of prognostic factors for Overall Survival.

Characteristic	Univariate HR (95% CI)	Univariate *p*-value	Multivariate HR (95% CI)	Multivariate *p*-value
Age (years)	0.997 (0.98–1.01)	0.764		
Gender (Male vs Female)	1.09 (0.655–1.83)	0.731		
Etiology (HCV vs HBV)	0.917 (0.537–1.57)	0.751		
Etiology (Other vs HBV)	1.22 (0.761–1.95)	0.411		
ECOG PS	0.92 (0.6–1.41)	0.703		
Tumor Size (cm)	1.13 (1.07–1.2)	<0.001	1.10 (1.04–1.16)	0.001
Tumor Number	1.25 (1.05–1.5)	0.014	1.34 (1.10–1.63)	0.003
Macrovascular Invasion (Yes vs No)	1.37 (0.916–2.04)	0.126	1.64 (1.08–2.48)	0.019
Extrahepatic Spread (Yes vs No)	1.03 (0.655–1.63)	0.889		
Log_{10}AFP	1.06 (0.65–1.74)	0.809		
ALBI Grade (Grade 2/3 vs 1)	3.2 (1.91–5.35)	<0.001	2.76 (1.62–4.70)	<0.001
Delta SII Group (High vs Low)	3.22 (2.15–4.84)	<0.001	2.84 (1.86–4.33)	<0.001

Univariate analysis included all baseline characteristics. Variables with a p-value < 0.10 in the univariate analysis, along with clinically relevant covariates, were considered for inclusion in the multivariate analysis. p-values < 0.05 were considered statistically significant in the multivariate model. Abbreviations: HR, Hazard Ratio; CI, Confidence Interval; ECOG PS, Eastern Cooperative Oncology Group Performance Status; MVI, Macrovascular Invasion; AFP, Alpha-fetoprotein; ALBI, Albumin-Bilirubin; SII, Systemic Immune-Inflammation Index.

by ALBI grade, significantly stratified patient prognosis (Fig. 1B). Patients with ALBI Grade 1 achieved superior OS ($p < 0.0001$) and PFS ($p = 0.0011$) compared to those with ALBI Grade 2 or 3. These results suggest that both the dynamic change in immune-inflammation status (Delta SII) and baseline liver function (ALBI grade) are robust determinants of survival in patients with unresectable HCC receiving TACE plus PD-1 inhibitors.

Identification of Independent Prognostic Factors

Univariate and multivariate Cox proportional hazards regression analyses were performed to identify predictors of overall survival (Table 2). In the univariate analysis, four variables were found to be statistically significant: Tumor Size ($p < 0.001$), Tumor Number ($p = 0.014$), ALBI Grade ($p < 0.001$), and Delta SII Group ($p < 0.001$).

Variables with $p < 0.10$ in the univariate analysis or with established clinical prognostic relevance were entered into the multivariate model. The analysis confirmed that Tumor Size (Hazard Ratio (HR): 1.10, 95% CI: 1.04–1.16, $p = 0.001$) was an independent prognostic factor. Tumor Number was also confirmed as an independent predictor (HR: 1.34, 95% CI: 1.10–1.63, $p = 0.003$), with its multivariable estimate modestly exceeding the univariate estimate (HR: 1.25). This pattern is consistent with a classical suppression effect: in the univariate model, Tumor Number implicitly absorbed a portion of the mortality risk more specifically attributable to MVI, a biologically correlated variable not yet controlled for, thereby attenuating its apparent effect size. Once MVI was independently adjusted for in the multivariable model, the true independent prognostic contribution of Tumor Number was more completely estimated, resulting in a slightly higher and more precise hazard ratio. This phenomenon does not indicate model instability, but rather reflects the expected consequence of appropriately adjusting for a biologically correlated covariate. More importantly, baseline hepatic reserve and dynamic immune status demonstrated robust predictive value. MVI was also identified as a prognostic factor (HR: 1.64, 95% CI: 1.08–2.48, $p = 0.019$). ALBI Grade 2/3 was associated with an approximately 2.8-fold increased risk of mortality compared to Grade 1 (HR: 2.76, 95% CI: 1.62–4.70, $p < 0.001$). Similarly, the High Delta-SII Group was identified as a powerful independent risk factor (HR: 2.84, 95% CI: 1.86–4.33, $p < 0.001$), suggesting that an increasing trend in SII during treatment is strongly indicative of poor prognosis. Multicollinearity among covariates in the multivariable Cox model was assessed using the variance inflation factor (VIF); all VIF values were below 1.1 (Delta SII: 1.039; ALBI Grade: 1.059; Tumor Size: 1.027; Tumor Number: 1.068; MVI: 1.057), confirming the absence of meaningful collinearity.

To evaluate potential information loss from the dichotomization of Delta SII, sensitivity analyses were performed using Delta SII as a continuous linear term and as a restricted cubic spline (RCS, 4 knots) in the multivariable Cox model. The nonlinearity test was non-significant ($p = 0.172$), indicating that the relationship between Delta SII and the log hazard of death is adequately captured by a linear function. The C-index of the continuous linear model (0.752, SE: 0.024) was virtually identical to that of the binary model (0.752, SE: 0.023), and although the continuous model achieved a marginally lower AIC (834.54 vs. 837.86 for the binary model), this did not translate into any meaningful gain in discriminative performance. These analyses confirm that dichotomization at the optimal cut-off of

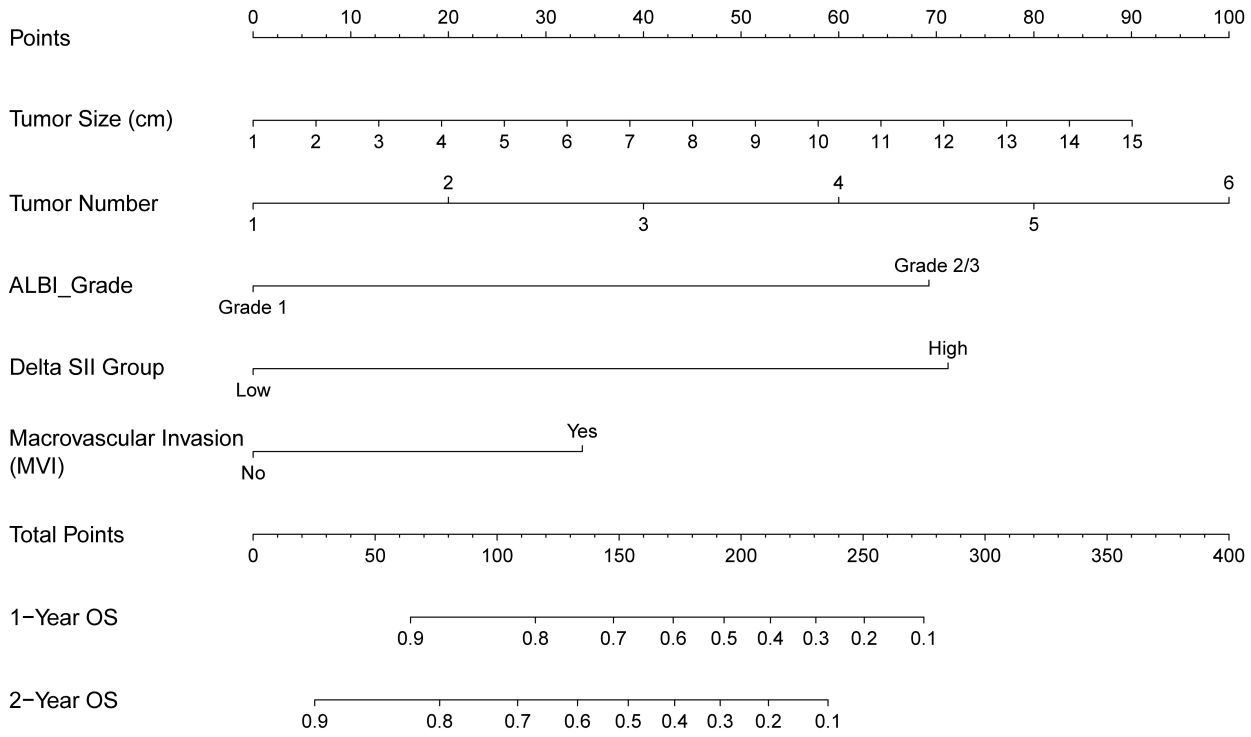

Fig. 2. Prognostic Nomogram for predicting 1- and 2-year Overall Survival (OS). The nomogram integrates five independent prognostic factors: Tumor Size, Tumor Number, MVI, ALBI Grade, and Delta SII Group. To use the nomogram, locate the patient's value for each variable on the corresponding axis, draw a vertical line up to the "Points" axis to determine the score, and sum the scores for all variables to obtain the "Total Points". The predicted 1-year and 2-year survival probabilities can be estimated by projecting the Total Points onto the bottom scales. Note: Delta SII Group and ALBI Grade demonstrate larger point ranges compared to tumor burden metrics, indicating their substantial contribution to the prognostic model. Abbreviations: ALBI, Albumin-Bilirubin; SII, Systemic Immune-Inflammation Index; OS, Overall Survival; MVI, Macrovascular Invasion.

32.7% does not result in clinically meaningful information loss, while offering the practical advantage of a directly actionable bedside threshold.

Construction and Validation of the Prognostic Nomogram

Based on the independent prognostic factors identified in the multivariate analysis including Tumor Size, Tumor Number, MVI, ALBI Grade, and Delta SII Group, a prognostic nomogram was established to predict 1- and 2-year Overall Survival (OS) (Fig. 2). In this visual model, each variable is assigned a specific score on the "Points" scale. By summing the scores of these five variables, the predicted survival probability can be determined. Notably, visual inspection of the nomogram reveals that the Delta SII Group and ALBI Grade make the largest contributions to the prognostic model (spanning the widest range on the point scale), followed by MVI, Tumor Size and Tumor Number. This underscores the critical impact of dynamic immune-inflammatory status and hepatic reserve on patient survival, which appears to outweigh the influence of tumor burden alone in this cohort.

The predictive performance of the nomogram was comprehensively validated using three methods:

(1) Discrimination: The time-dependent ROC analysis yielded an Area Under the Curve (AUC) of 0.804 (95% CI: 0.737–0.872) for 1-year OS and 0.823 (95% CI: 0.756–0.890) for 2-year OS (Fig. 3A), both indicative of good-to-excellent discriminative performance. Notably, the 2-year AUC was meaningfully higher than the 1-year AUC, the point estimates are consistently higher at 2 years, suggesting a progressive improvement in predictive accuracy rather than a chance variation. This progressive improvement in predictive accuracy over time diverges from the typical decay pattern observed in conventional chemotherapy-based prognostic models. We attribute this phenomenon to the biological nature of the two incorporated host factors: Delta SII and ALBI grade are determinants of durable immunological response and hepatic resilience, which become increasingly decisive for survival beyond the first year of immunotherapy, consistent with the characteristic "long-tail" survival pattern of checkpoint inhibitor-based treatment [24]. In contrast, short-term mortality within the first year is more heavily influenced by acute events, such as

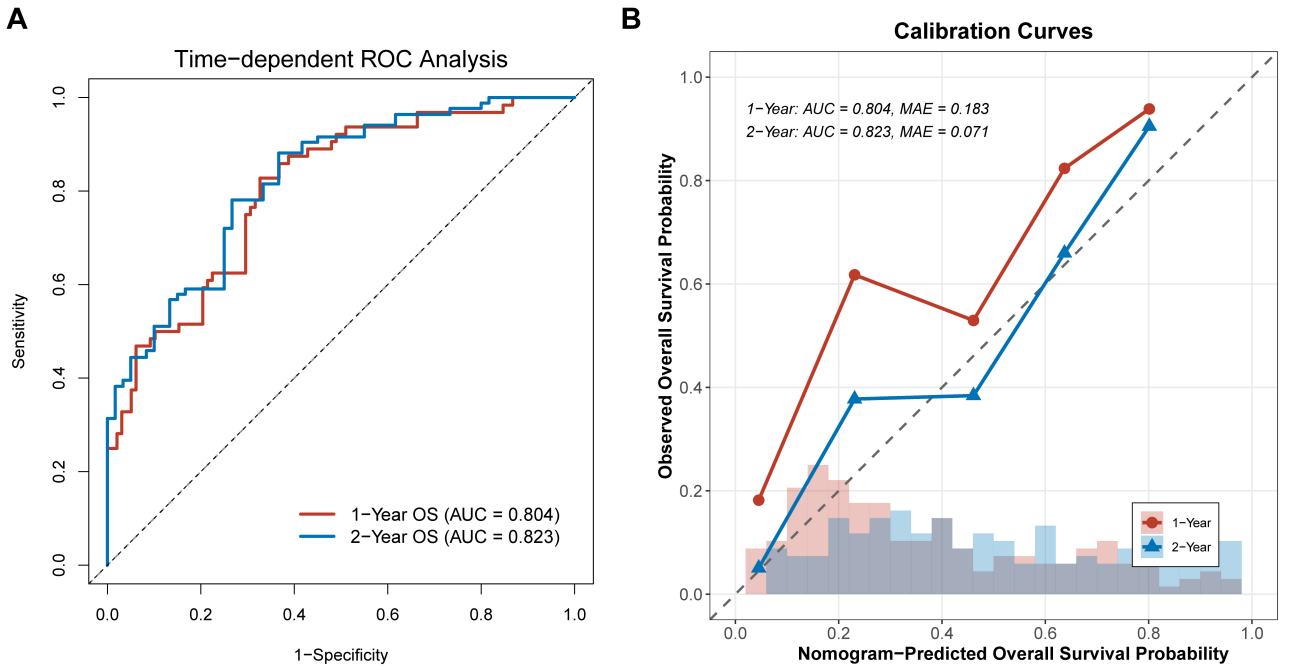

Fig. 3. Validation of the Nomogram. (A) Time-dependent ROC analysis. The ROC curves for 1-year (red line) and 2-year (blue line) Overall Survival. The AUC values were 0.804 (95% CI: 0.737–0.872) and 0.823 (95% CI: 0.756–0.890), respectively, indicating good discrimination. (B) Calibration curves. The calibration plots for 1-year (red) and 2-year (blue) Overall Survival. The x-axis represents the nomogram-predicted survival probability, and the y-axis represents the actual observed survival probability. The diagonal dashed line represents ideal prediction. The text box displays the AUC and Mean Absolute Error (MAE) for each time point. Abbreviations: ROC, Receiver Operating Characteristic; AUC, Area Under the Curve.

post-TACE liver failure or early refractory tumor progression, that are less precisely captured by these biological markers. To further demonstrate the incremental value of the nomogram over individual components, a comparative analysis against ALBI grade alone and tumor burden alone is presented in **Supplementary Tables 1**,**2**.

(2) Calibration: The calibration curves for 1- and 2-year OS revealed high consistency between the nomogram-predicted probabilities and the actual observed survival rates (Fig. 3B). The Mean Absolute Error (MAE) was 0.183 for 1-year prediction and 0.071 for 2-year prediction, indicating that the model fits the data well.

(3) Clinical Utility: Decision Curve Analysis (DCA) was performed to assess the net benefit of the nomogram. As shown in Fig. 4, the nomogram (solid lines) provided a higher net benefit compared to the "treat-all" (dashed lines) or "treat-none" strategies across a wide range of threshold probabilities for both 1- and 2-year predictions. This confirms the practical value of the nomogram in guiding clinical decision-making.

Discussion

The advent of ICIs combined with locoregional therapies, such as TACE, has revolutionized the treatment landscape for unresectable HCC. Despite these advances, the heterogeneity in therapeutic response remains a formidable clinical challenge. In this retrospective study, we constructed and validated a novel nomogram integrating tumor burden, hepatic reserve (ALBI grade), and dynamic immune-inflammatory changes (Delta SII). The model demonstrated robust predictive accuracy, particularly for long-term survival (2-year OS), highlighting a critical paradigm shift: in the era of immunotherapy, the patient's systemic immune status and hepatic resilience may outweigh conventional tumor morphological characteristics in determining outcomes.

A striking finding from our nomogram (Fig. 2) is the hierarchical contribution of prognostic factors. Visual inspection of the point scales reveals that biological and functional markers (Delta SII Group and ALBI Grade) span a wider range of "Points" compared to morphological metrics like Tumor Size and Tumor Number. Traditionally, staging systems such as the BCLC have relied heavily on tumor burden to dictate prognosis [25]. However, our results suggest that for patients undergoing combination immunotherapy, the "host factor", specifically the immuno-hepatic mi-

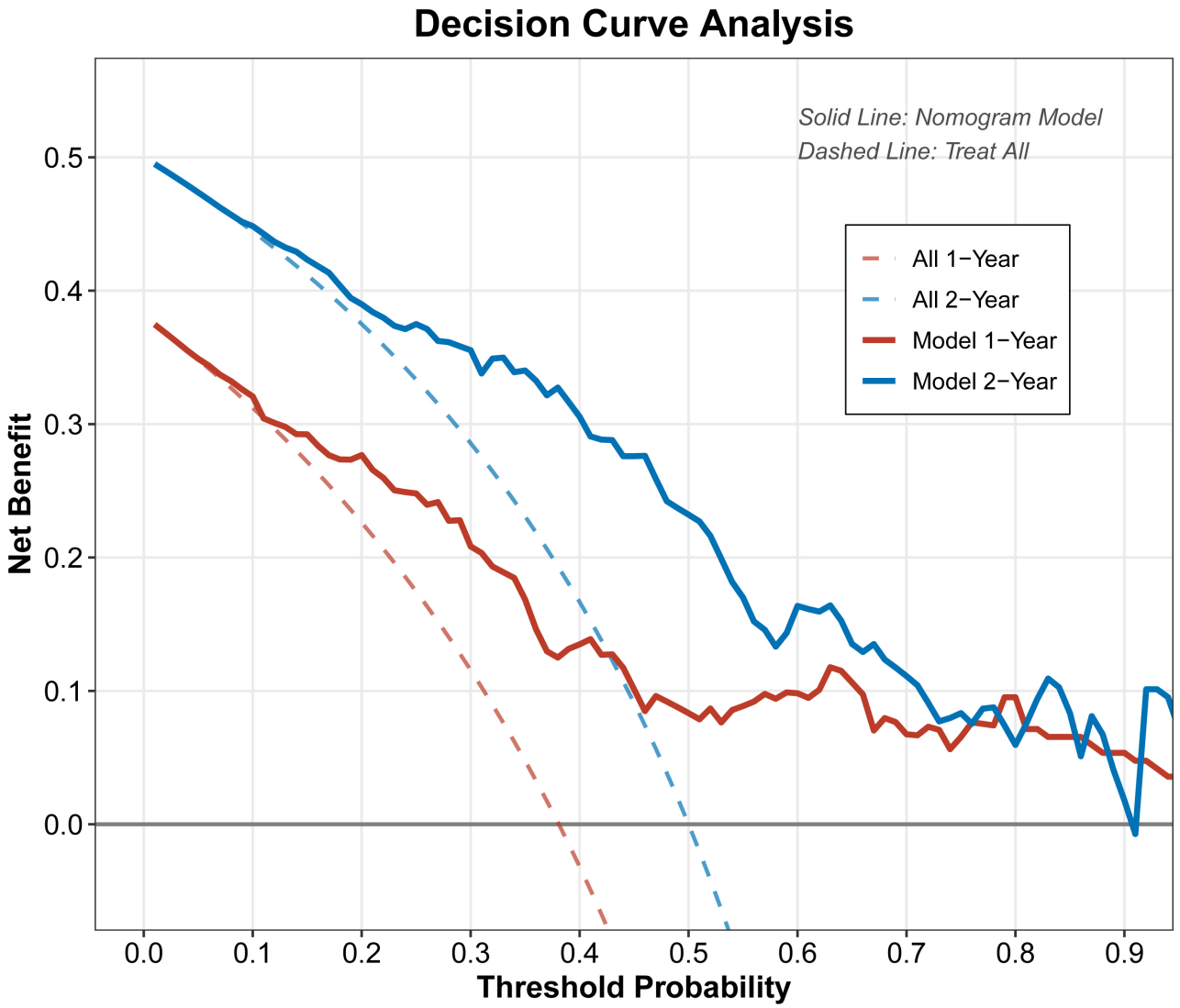

Fig. 4. Decision Curve Analysis (DCA). DCA for the nomogram predicting 1-year (red) and 2-year (blue) Overall Survival. The y-axis measures the net benefit. The solid lines represent the nomogram model. The dashed lines represent the assumption that all patients experience the event ("Treat All"). The grey horizontal line represents the assumption that no patients experience the event ("Treat None"). The model showed positive net benefit across a wide range of threshold probabilities, indicating its clinical utility.

croenvironment, plays a more decisive role than the tumor burden alone. This observation aligns with the mechanism of PD-1 inhibitors, which rely on reinvigorating the host's existing immune cells rather than directly targeting cancer cells [26,27]. Consequently, a patient harboring a smaller tumor but with exhausted immune status (High Delta SII) or compromised hepatic function (ALBI 2/3) may carry a worse prognosis than one with a larger tumor burden but an intact immune profile.

Liver function reserve remains the cornerstone of survival in HCC [28]. Unlike the Child-Pugh score, which incorporates subjective variables, the ALBI grade offers a strictly objective assessment of hepatic function [29]. Our multivariate analysis confirmed that ALBI grade 2/3 is a potent risk factor. This is biologically plausible, as TACE induces ischemic necrosis, inevitably causing transient hepatic impairment [30]. In patients with limited functional reserve (ALBI 2/3), this procedure-related stress, combined with potential immune-mediated hepatotoxicity (IMH) from PD-1 inhibitors, can precipitate liver failure or prevent the administration of subsequent treatment cycles [31]. As shown in our Kaplan-Meier analysis (Fig. 1B), the separation between ALBI Grade 1 and 2/3 is distinct and sustained, confirming that preserving liver function is as crucial as controlling the tumor.

Beyond hepatic reserve, the dynamic evolution of the SII proved to be a superior predictor compared to static baseline values. While baseline SII failed to stratify risk in our cohort, an increasing SII (High Delta-SII) during treatment was strongly associated with poor OS and PFS

(Fig. 1A). Mechanistically, this dynamic change likely reflects the interplay between TACE-induced hypoxia and the immune response. TACE creates an ischemic tumor microenvironment that upregulates Hypoxia-Inducible Factor 1-alpha (HIF-1α), leading to the secretion of VEGF and pro-inflammatory cytokines [32,33].

Moreover, the absence of a prognostic signal from baseline SII, in contrast to the strong predictive value of Delta SII, warrants mechanistic explanation. Baseline SII reflects a patient's chronic, pre-treatment inflammatory steady state, which was relatively homogeneous in our cohort given the Child-Pugh A/B inclusion criterion. In contrast, Delta SII captures the magnitude of the acute inflammatory perturbation triggered by TACE through three simultaneous biological processes. First, TACE-induced ischemic necrosis upregulates HIF-1α, driving a surge in pro-inflammatory cytokines which stimulate emergency granulopoiesis and megakaryocyte proliferation, elevating the SII numerator. Second, TACE-induced endothelial injury triggers rapid platelet activation, with released TGF-β suppressesing lymphocyte effector function and reducing the SII denominator. Third, TACE-induced ischemia-reperfusion injury exacerbates splenic sequestration of lymphocytes in patients with compromised hepatic reserve. Patients with insufficient biological resilience exhibit a persistently elevated SII, whereas immunologically robust patients demonstrate efficient inflammatory resolution. Delta SII therefore serves as a composite real-time readout of host biological resilience under therapeutic stress, a dimension of prognostic information invisible to any single time-point measurement. It is this differential capacity for inflammatory resolution that ultimately determines the host's ability to sustain durable anti-tumor immunity under PD-1 blockade.

Furthermore, in the context of a high Delta-SII, platelets and neutrophils act as synergistic contributors in tumor progression [34,35]. Activated platelets release high levels of Transforming Growth Factor-beta (TGF-β), which impairs CD8+ T-cell effector function and directly antagonizes the therapeutic mechanism of PD-1 inhibitors [36–38]. Simultaneously, platelets form a physical barrier around circulating tumor cells, shielding them from natural killer (NK) cell-mediated lysis and promoting metastasis [39–41]. Concurrently, neutrophils release Neutrophil Extracellular Traps (NETs) that sequester tumor cells and protect them from cytotoxic T lymphocytes [42]. Thus, a rising SII essentially signals the formation of a pro-tumorigenic niche that physically and chemically blocks the anti-tumor immunity induced by PD-1 inhibitors.

Intriguingly, our baseline characteristic analysis (Table 1) unveiled a significant correlation between the High Delta-SII group and poorer hepatic parameters (higher total bilirubin and ALBI Grade 2/3), despite comparable baseline SII levels. This observation points to a mechanistically plausible "vicious cycle" between systemic inflammation and hepatic decompensation that operates through several interconnected pathways.

This correlation points to a bidirectional amplification loop between hepatic dysfunction and systemic inflammation. On one hand, advanced liver dysfunction promotes lymphocyte sequestration via portal hypertension-driven hypersplenism and sustains neutrophilia through chronic bacterial translocation and elevated pro-inflammatory cytokines (IL-6, TNF-α), thereby elevating the SII [43–47]. On the other hand, in the context of TACE-induced ischemia-reperfusion injury, activated neutrophils release reactive oxygen species (ROS) and proteolytic enzymes that inflict direct parenchymal damage, while platelet-derived TGF-β1 promotes hepatic fibrogenesis, further compromising hepatic reserve [36,48]. This bidirectional amplification loop explains why patients with pre-existing ALBI Grade 2/3 are biologically predisposed to an exaggerated and sustained inflammatory surge following TACE, making Delta SII a composite surrogate of the host's overall physiological resilience rather than a purely immunological marker.

A legitimate concern is whether High Delta SII merely reflects a more advanced disease state, characterized by greater tumor burden and more compromised hepatic reserve, rather than constituting an independent biological risk factor. Several lines of evidence argue against a purely epiphenomenal interpretation. First, in the multivariable Cox regression model, Delta SII retained its independent prognostic significance (HR: 2.84, 95% CI: 1.86–4.33) after simultaneous adjustment for tumor size, tumor number, and ALBI grade, indicating that its predictive value is not simply a proxy for these established risk factors. Second, and critically, baseline SII, which was measured at the same clinical severity state as ALBI grade and tumor burden, showed no significant difference between groups (p = 0.886) and failed to stratify prognosis in our cohort. This dissociation between baseline SII and Delta SII directly demonstrates that it is the treatment-induced dynamic change in systemic immune-inflammation, rather than the static level of pre-existing disease severity, that confers independent prognostic information. Third, the interaction between TACE-induced ischemic stress and the host immune-inflammatory response is a biologically distinct event that occurs after treatment initiation and therefore cannot be fully anticipated or subsumed by pre-treatment staging metrics. Collectively, these findings support Delta SII as a genuinely independent, treatment-responsive biomarker rather than a surrogate of baseline disease burden.

A unique strength of our nomogram is its time-dependent performance characteristics. As illustrated in the time-dependent ROC analysis (Fig. 3A), the AUC for 2-year OS (0.823) was noticeably superior to that for 1-year OS (0.804). This phenomenon diverges from traditional chemotherapy models, where predictive accuracy typically

decays over time, but it is highly consistent with the "long-tail effect" characteristic of immunotherapy survival curves [24]. Short-term mortality (1-year) in this population is more heavily influenced by acute procedural events, such as post-TACE hepatic decompensation or early refractory tumor progression, which are inherently less well captured by biological markers of host immune and hepatic reserve. As a result, the prognostic signal contributed by Delta SII and ALBI grade is partially diluted at the 1-year landmark by these acute confounders. In contrast, long-term survival beyond one year becomes increasingly contingent upon the patient's durable immunological capacity and hepatic resilience, domains that Delta SII and ALBI grade are specifically designed to reflect. Our nomogram, by heavily weighting Delta SII and ALBI, effectively captures these determinants of long-term stability. The excellent calibration curves (Fig. 3B) further validate that our model accurately predicts these probabilities without significant overfitting. The relatively higher calibration error at 1 year (MAE: 0.183) compared to 2 years (MAE: 0.071) may reflect the limited number of early mortality events available for 1-year calibration estimation, as well as the greater influence of acute treatment-related confounders in the short-term survival trajectory.

However, statistical significance does not always translate to clinical utility. To address this, we employed Decision Curve Analysis (DCA). As shown in Fig. 4, the nomogram provided a net benefit superior to both the "treat-all" and "treat-none" strategies across a wide range of threshold probabilities (approximately 20% to 80%). This wide actionable range indicates that the model is clinically useful for diverse decision-making scenarios. For instance, in patients with a high predicted mortality risk (High Delta SII + ALBI 2/3), clinicians might consider closer radiologic surveillance, earlier switch to systemic monotherapy to avoid TACE-induced liver damage, or enrollment in clinical trials testing alternative mechanisms of action. The modest increase in the HR for Tumor Number from univariate (HR: 1.25) to multivariable analysis (HR: 1.34) reflects a suppression effect attributable to the collinearity between Tumor Number and MVI. In the univariate model, part of the mortality risk specific to MVI was implicitly absorbed by Tumor Number; once MVI was independently controlled for in the multivariable model, the true independent prognostic contribution of Tumor Number was more completely estimated.

This study has several limitations that should be considered when interpreting the findings. First, the retrospective single-institution design limits external generalizability, and the absence of an independent external validation cohort remains a significant drawback; we attempted to mitigate this through rigorous 500-bootstrap internal validation and confirmation of adequate events per variable. Second, as a consequence of the retrospective data collection approach, three treatment-related variables were not systematically documented: the specific TACE modality (cTACE vs. DEB-TACE), the cumulative number of TACE sessions administered, and the proportion of patients receiving concomitant tyrosine kinase inhibitors. Nevertheless, we note that the primary prognostic determinants in our model (ALBI grade and Delta SII) reflect intrinsic hepatic functional reserve and systemic immune-inflammatory balance, respectively. These are host biological characteristics that are established prior to and independently of any specific pharmacological co-intervention, making them less susceptible to directional confounding by TKI co-administration. While we cannot formally exclude a degree of residual confounding, the directional validity of the reported prognostic associations is unlikely to be fundamentally altered. Future prospective studies should prespecify and document concomitant systemic therapies to allow formal interaction testing.

While we acknowledge that these unmeasured variables represent potential sources of residual confounding, several considerations suggest that TACE modality heterogeneity is unlikely to fundamentally invalidate the core findings. First, modality selection in our cohort was driven by objective tumor vascular anatomy: tumors with well-defined hypervascular feeders were more likely to receive DEB-TACE, whereas those with complex or diffuse vascularity received cTACE. This anatomical selection criterion is not systematically correlated with ALBI grade or Delta SII, both of which reflect intrinsic host physiology rather than tumor vascularity. Second, published meta-analyses have not demonstrated significant differences in overall survival between cTACE and DEB-TACE in unresectable HCC, suggesting that modality heterogeneity is unlikely to exert a directional bias on survival outcomes in the present cohort. These unmeasured variables represent potential sources of treatment heterogeneity that could not be formally adjusted for in the multivariable model. While we believe the core prognostic associations of ALBI grade and Delta SII are biologically robust (given that both markers reflect intrinsic host physiology rather than procedure-level technical factors) we cannot exclude a degree of residual confounding. Third, the cohort exclusively received toripalimab as the PD-1 inhibitor. While this reduces pharmacological heterogeneity within the study, it limits the direct applicability of the nomogram to settings where alternative PD-1 inhibitors are employed. Future prospective multicenter studies should prespecify TACE modality, cumulative treatment cycles, and concomitant systemic therapies as stratification or adjustment variables, and should enroll patients across multiple PD-1 inhibitor regimens to establish the broader generalizability of these findings.

Furthermore, the exact blood draw date relative to the treatment cycle was not systematically recorded in the retrospective dataset, precluding a formal quantitative sensitivity analysis of intra-window sampling timing effects on Delta SII; this should be addressed in future prospec-

tive studies. Also, radiological progression was assessed through routine clinical review rather than formal blinded independent dual-reader evaluation, which may introduce a degree of ascertainment variability; prospective studies should prespecify a blinded central imaging review process. Additionally, the total number of initially screened patients could not be precisely ascertained due to the absence of a prospective screening log during the study period, which limits full enrollment transparency; future prospective studies should maintain formal screening logs in accordance with STROBE reporting guidelines.

Conclusion

In conclusion, the dynamic change in SII, combined with ALBI grade, serves as a powerful prognostic tool for unresectable HCC patients receiving TACE plus PD-1 inhibitors. We developed a user-friendly nomogram that visually prioritizes biological function over tumor morphology. This tool shows exceptional performance in predicting long-term survival, offering clinicians a practical guide to identify patients who are most likely to achieve durable benefits from this combination therapy.

Availability of Data and Materials

The data that support the findings of this study are available from the corresponding author upon reasonable request.

Author Contributions

YJP and JW designed the research study. YJP and FH performed the research. XYW and TL analyzed the data. JW drafted the article. All authors contributed to important editorial changes in the manuscript. All authors read and approved the final manuscript. All authors have participated sufficiently in the work and agreed to be accountable for all aspects of the work.

Ethics Approval and Consent to Participate

This study was conducted in accordance with the Declaration of Helsinki and was approved by the Institutional Review Board (IRB) of People's Hospital of Ningxia Hui Autonomous Region (Approval No. [2025]-NZR-229). Given the retrospective nature of the study and the use of anonymized clinical data, the requirement for written informed consent was waived. The study is reported in line with the STROBE statement for observational studies and the TRIPOD guideline for prognostic model development and validation.

Acknowledgment

Not applicable.

Funding

This research received no external funding.

Conflict of Interest

The authors declare no conflict of interest.

Supplementary Material

Supplementary material associated with this article can be found, in the online version, at https://doi.org/10.24976/Discov.Med.202638207.95.

References

[1] Singh SP, Madke T, Chand P. Global Epidemiology of Hepatocellular Carcinoma. Journal of Clinical and Experimental Hepatology. 2025; 15: 102446. https://doi.org/10.1016/j.jceh.2024.102446.

[2] Kale SR, Karande G, Gudur A, Garud A, Patil MS, Patil S. Recent Trends in Liver Cancer: Epidemiology, Risk Factors, and Diagnostic Techniques. Cureus. 2024; 16: e72239. https://doi.org/10.7759/cureus.72239.

[3] Jin K, Zeng S, Li B, Zhang G, Wu J, Hu X, *et al*. Bicarbonate-integrated transarterial chemoembolization (TACE) in real-world hepatocellular carcinoma. Signal Transduction and Targeted Therapy. 2025; 10: 281. https://doi.org/10.1038/s41392-025-02400-x.

[4] Lee M, Shin HP. Efficacy of Transarterial Chemoembolization (TACE) for Early-Stage Hepatocellular Carcinoma. Medicina (Kaunas, Lithuania). 2023; 59: 2174. https://doi.org/10.3390/medicina59122174.

[5] Xu W, Weng J, Zhao Y, Xie P, Xu M, Liu S, *et al*. FMO2^{+} cancer-associated fibroblasts sensitize anti-PD-1 therapy in patients with hepatocellular carcinoma. Journal for Immunotherapy of Cancer. 2025; 13: e011648. https://doi.org/10.1136/jitc-2025-011648.

[6] Li L, Xu X, Wang W, Huang P, Yu L, Ren Z, *et al*. Safety and efficacy of PD-1 inhibitor (sintilimab) combined with transarterial chemoembolization as the initial treatment in patients with intermediate-stage hepatocellular carcinoma beyond up-to-seven criteria. Journal for Immunotherapy of Cancer. 2025; 13: e010035. https://doi.org/10.1136/jitc-2024-010035.

[7] Sun W, Liu Y, Wang L. Feasibility and Safety of the Clinical Outcomes of TACE Combined with Lenvatinib and PD-1 Blockades in the Treatment of Hepatocellular Carcinoma with Portal Vein Tumor Thrombus: A Retrospective Exploratory Study. International Journal of General Medicine. 2024; 17: 3627–3640. https://doi.org/10.2147/IJGM.S473676.

[8] Chen Y, Deng X, Li Y, Han Y, Peng Y, Wu W, *et al*. Comprehensive molecular classification predicted microenvironment profiles and therapy response for HCC. Hepatology (Baltimore, Md.). 2024; 80: 536–551. https://doi.org/10.1097/HEP.0000000000000869.

[9] Liapis I, Ziogas IA, Theocharopoulos C, Moris DP, Nydam TL, Gleisner AL, *et al*. Re-evaluating surgical strategies in Barcelona Clinic Liver Cancer-B hepatocellular carcinoma. World Journal of Hepatology. 2025; 17: 108970. https://doi.org/10.4254/wjh.v17.i9.108970.

[10] Kohla M, Ashour R, Taha H, El-Abd O, Osman M, Abozeid M, *et al*. Prognostic performance of Hong Kong Liver Cancer with Barcelona Clinic Liver Cancer staging systems in hepatocellular

carcinoma. BMC Gastroenterology. 2024; 24: 318. https://doi.org/10.1186/s12876-024-03387-5.

[11] Mandlik DS, Mandlik SK, Choudhary HB. Immunotherapy for hepatocellular carcinoma: Current status and future perspectives. World Journal of Gastroenterology. 2023; 29: 1054–1075. https://doi.org/10.3748/wjg.v29.i6.1054.

[12] Li Q, Han J, Yang Y, Chen Y. PD-1/PD-L1 checkpoint inhibitors in advanced hepatocellular carcinoma immunotherapy. Frontiers in Immunology. 2022; 13: 1070961. https://doi.org/10.3389/fimmu.2022.1070961.

[13] Celsa C, Cabibbo G, Fulgenzi CAM, Battaglia S, Enea M, Scheiner B, *et al*. Hepatic decompensation is the major driver of mortality in patients with HCC treated with atezolizumab plus bevacizumab: The impact of successful antiviral treatment. Hepatology (Baltimore, Md.). 2025; 81: 837–852. https://doi.org/10.1097/HEP.0000000000001026.

[14] Yang L, Zhu H, Zhang X, Fu X, Zhao X, Wang X, *et al*. Evaluation of hepatic functional reserve of hepatocellular carcinoma ($\leq$ 5 cm) by liver shear wave velocity combined with multiple parameters. Frontiers in Oncology. 2024; 14: 1301052. https://doi.org/10.3389/fonc.2024.1301052.

[15] da Fonsecaa LG, de Melob MAZ, da Silveirac THM, Yamamotod VJ, Hashizumee PHS, Sabbagaf J. Prognostic role of albumin-bilirubin (ALBI) score and Child-Pugh classification in patients with advanced hepatocellular carcinoma under systemic treatment. Ecancermedicalscience. 2024; 18: 1748. https://doi.org/10.3332/ecancer.2024.1748.

[16] Bannangkoon K, Hongsakul K, Tubtawee T, Ina N. Prognostic Value of Myosteatosis and Albumin-Bilirubin Grade for Survival in Hepatocellular Carcinoma Post Chemoembolization. Cancers. 2024; 16: 3503. https://doi.org/10.3390/cancers16203503.

[17] Nishida A, Andoh A. The Role of Inflammation in Cancer: Mechanisms of Tumor Initiation, Progression, and Metastasis. Cells. 2025; 14: 488. https://doi.org/10.3390/cells14070488.

[18] Li D, Zhao X, Pi X, Wang K, Song D. Systemic immune-inflammation index and the survival of hepatocellular carcinoma patients after transarterial chemoembolization: a meta-analysis. Clinical and Experimental Medicine. 2023; 23: 2105–2114. https://doi.org/10.1007/s10238-022-00889-y.

[19] Tan S, Zheng Q, Zhang W, Zhou M, Xia C, Feng W. Prognostic value of inflammatory markers NLR, PLR, and LMR in gastric cancer patients treated with immune checkpoint inhibitors: a meta-analysis and systematic review. Frontiers in Immunology. 2024; 15: 1408700. https://doi.org/10.3389/fimmu.2024.1408700.

[20] Nakamoto S, Ohtani Y, Sakamoto I, Hosoda A, Ihara A, Naitoh T. Systemic Immune-Inflammation Index Predicts Tumor Recurrence after Radical Resection for Colorectal Cancer. The Tohoku Journal of Experimental Medicine. 2023; 261: 229–238. https://doi.org/10.1620/tjem.2023.J074.

[21] Lin XH, Qiu BQ, Ma M, Zhang R, Hsu SJ, Liu HH, *et al*. Suppressing DRP1-mediated mitochondrial fission and mitophagy increases mitochondrial apoptosis of hepatocellular carcinoma cells in the setting of hypoxia. Oncogenesis. 2020; 9: 67. https://doi.org/10.1038/s41389-020-00251-5.

[22] Mallick S, K N A, Sivaprasadan S, S S. Immunosuppression in Liver Transplant Recipients in the Setting of Sepsis. Journal of Clinical and Experimental Hepatology. 2023; 13: 682–690. https://doi.org/10.1016/j.jceh.2022.10.012.

[23] Reig M, Forner A, Rimola J, Ferrer-Fàbrega J, Burrel M, Garcia-Criado Á, *et al*. BCLC strategy for prognosis prediction and treatment recommendation: The 2022 update. Journal of Hepatology. 2022; 76: 681–693. https://doi.org/10.1016/j.jhep.2021.11.018.

[24] Higham CE, Chatzimavridou-Grigoriadou V, Fitzgerald CT, Trainer PJ, Eggermont AMM, Lorigan P. Adjuvant immunotherapy: the sting in the tail. European Journal of Cancer (Oxford, England: 1990). 2020; 132: 207–210. https://doi.org/10.1016/j.ejca.2020.03.016.

[25] Tümen D, Heumann P, Gülow K, Demirci CN, Cosma LS, Müller M, *et al*. Pathogenesis and Current Treatment Strategies of Hepatocellular Carcinoma. Biomedicines. 2022; 10: 3202. https://doi.org/10.3390/biomedicines10123202.

[26] Grippin AJ, Marconi C, Copling S, Li N, Braun C, Woody C, *et al*. SARS-CoV-2 mRNA vaccines sensitize tumours to immune checkpoint blockade. Nature. 2025; 647: 488–497. https://doi.org/10.1038/s41586-025-09655-y.

[27] Pauken KE, Torchia JA, Chaudhri A, Sharpe AH, Freeman GJ. Emerging concepts in PD-1 checkpoint biology. Seminars in Immunology. 2021; 52: 101480. https://doi.org/10.1016/j.smim.2021.101480.

[28] Miki A, Sakuma Y, Watanabe J, Endo K, Sasanuma H, Teratani T, *et al*. Remnant liver function is associated with long-term survival in patients with hepatocellular carcinoma undergoing hepatectomy. Scientific Reports. 2023; 13: 15637. https://doi.org/10.1038/s41598-023-42929-x.

[29] Demirtas CO, D'Alessio A, Rimassa L, Sharma R, Pinato DJ. ALBI grade: Evidence for an improved model for liver functional estimation in patients with hepatocellular carcinoma. JHEP Reports: Innovation in Hepatology. 2021; 3: 100347. https://doi.org/10.1016/j.jhepr.2021.100347.

[30] Liu Y, Liu J, Zheng C, Ma Z. Recent Advances in Embolic Agents for Transarterial Chemoembolization of Hepatocellular Carcinoma. Advanced Healthcare Materials. 2026; 15: e02566. https://doi.org/10.1002/adhm.202502566.

[31] Li X, Ji L, Li X, Sun D, Yang W. Application of artificial liver in immune-related liver injury induced by immune checkpoint inhibitor: Case reports and review of the literature. Frontiers in Immunology. 2022; 13: 1001823. https://doi.org/10.3389/fimmu.2022.1001823.

[32] Chung SW, Kim JS, Choi WM, Choi J, Lee D, Shim JH, *et al*. Synergistic Effects of Transarterial Chemoembolization and Lenvatinib on HIF-1α Ubiquitination and Prognosis Improvement in Hepatocellular Carcinoma. Clinical Cancer Research: an Official Journal of the American Association for Cancer Research. 2025; 31: 2046–2055. https://doi.org/10.1158/1078-0432.CCR-24-1228.

[33] Pinto E, Pelizzaro F, Cardin R, Battistel M, Palano G, Bertellini F, *et al*. HIF-1α and VEGF as prognostic biomarkers in hepatocellular carcinoma patients treated with transarterial chemoembolization. Digestive and Liver Disease: Official Journal of the Italian Society of Gastroenterology and the Italian Association for the Study of the Liver. 2024; 56: 872–879. https://doi.org/10.1016/j.dld.2023.09.019.

[34] Langiu M, Palacios-Acedo AL, Crescence L, Mege D, Dubois C, Panicot-Dubois L. Neutrophils, Cancer and Thrombosis: The New Bermuda Triangle in Cancer Research. International Journal of Molecular Sciences. 2022; 23: 1257. https://doi.org/10.3390/ijms23031257.

[35] Yang W, Zheng X, Wu M, Zhang F, Xu S, Wang X, *et al*. Development and validation of postoperative and preoperative platelets ratio (PPR) to predict the prognosis of patients undergoing surgery for colorectal cancer: A dual-center retrospective cohort study. Cancer Medicine. 2023; 12: 111–121. https://doi.org/10.1002/cam4.4930.

[36] Lu M, Gong X, Zhang YM, Guo YW, Zhu Y, Zeng XB, *et al*. Platelets promote primary hepatocellular carcinoma metastasis through TGF-β1-mediated cancer cell autophagy. Cancer Letters. 2024; 600: 217161. https://doi.org/10.1016/j.canlet.2024.217161.

[37] Derynck R, Turley SJ, Akhurst RJ. TGFβ biology in can-

cer progression and immunotherapy. Nature Reviews. Clinical Oncology. 2021; 18: 9–34. https://doi.org/10.1038/s41571-020-0403-1.

[38] Mariathasan S, Turley SJ, Nickles D, Castiglioni A, Yuen K, Wang Y, *et al*. TGFβ attenuates tumour response to PD-L1 blockade by contributing to exclusion of T cells. Nature. 2018; 554: 544–548. https://doi.org/10.1038/nature25501.

[39] Li S, Lu Z, Wu S, Chu T, Li B, Qi F, *et al*. The dynamic role of platelets in cancer progression and their therapeutic implications. Nature Reviews. Cancer. 2024; 24: 72–87. https://doi.org/10.1038/s41568-023-00639-6.

[40] Placke T, Örgel M, Schaller M, Jung G, Rammensee HG, Kopp HG, *et al*. Platelet-derived MHC class I confers a pseudonormal phenotype to cancer cells that subverts the antitumor reactivity of natural killer immune cells. Cancer Research. 2012; 72: 440–448. https://doi.org/10.1158/0008-5472.CAN-11-1872.

[41] Lu Y, Lian S, Ye Y, Yu T, Liang H, Cheng Y, *et al*. S-Nitrosocaptopril prevents cancer metastasis in vivo by creating the hostile bloodstream microenvironment against circulating tumor cells. Pharmacological Research. 2019; 139: 535–549. https://doi.org/10.1016/j.phrs.2018.10.020.

[42] Wang H, Kim SJ, Lei Y, Wang S, Wang H, Huang H, *et al*. Neutrophil extracellular traps in homeostasis and disease. Signal Transduction and Targeted Therapy. 2024; 9: 235. https://doi.org/10.1038/s41392-024-01933-x.

[43] Yoshida H, Shimizu T, Yoshioka M, Matsushita A, Kawano Y, Ueda J, *et al*. The Role of the Spleen in Portal Hypertension. Journal of Nippon Medical School = Nippon Ika Daigaku Zasshi. 2023; 90: 20–25. https://doi.org/10.1272/jnms.JNMS.2023_90-104.

[44] Rodríguez-Negrete EV, Gálvez-Martínez M, Sánchez-Reyes K, Fajardo-Felix CF, Pérez-Reséndiz KE, Madrigal-Santillán EO, *et al*. Liver Cirrhosis: The Immunocompromised State. Journal of Clinical Medicine. 2024; 13: 5582. https://doi.org/10.3390/jcm13185582.

[45] Lu K, Shi TS, Shen SY, Shi Y, Gao HL, Wu J, *et al*. Defects in a liver-bone axis contribute to hepatic osteodystrophy disease progression. Cell Metabolism. 2022; 34: 441–457.e7. https://doi.org/10.1016/j.cmet.2022.02.006.

[46] Webb CE, Vautrinot J, Hers I. IL-6 as a Mediator of Platelet Hyper-Responsiveness. Cells. 2025; 14: 766. https://doi.org/10.3390/cells14110766.

[47] Chu T, Hu S, Qi J, Li X, Zhang X, Tang Y, *et al*. Bifunctional effect of the inflammatory cytokine tumor necrosis factor α on megakaryopoiesis and platelet production. Journal of Thrombosis and Haemostasis: JTH. 2022; 20: 2998–3010. https://doi.org/10.1111/jth.15891.

[48] Liu R, Cao H, Zhang S, Cai M, Zou T, Wang G, *et al*. ZBP1-mediated apoptosis and inflammation exacerbate steatotic liver ischemia/reperfusion injury. The Journal of Clinical Investigation. 2024; 134: e180451. https://doi.org/10.1172/JCI180451.